Ann. Acad. Rom. Sci.
Ser. Math. Appl.
ISSN 2066-6594 Vol. 14, No. 1-2/2022

DYNAMIC MODE DECOMPOSITION:A NEW APPROACH FOR COMPUTING THE DMD MODES AND EIGENVALUES*

Gyurhan H. Nedzhibov†

Abstract

Dynamic mode decomposition is a relatively recent development in the field of modal decompositions, however, it is a commonly used technique for analyzing the dynamics of nonlinear systems. Its success is due to the fact that it is an equation-free, data-driven method capable of providing accurate assessments of the spatiotemporal coherent structures in a complex system, or short-time future estimates. The aim of this work is to present a new approach for computing the dynamic mode decomposition. We show that our algorithm is closely related to the currently accepted algorithm. In fact, the two approaches produce the same DMD eigenvalues, it is only the DMD modes that differ. We demonstrate the new approach on two examples model systems.

MSC: 65P02, 37M02, 37L65

keywords: Dynamic mode decomposition, Koopman operator, Frobenius companion matrix, Singular value decomposition, Equation-free.

*Accepted for publication on June 22-th, 2021

†g.nedzhibov@shu.bg Faculty of Mathematics and Informatics, Shumen University, Shumen 9700, Bulgaria; Paper written with financial support of Shumen University under Grant RD-08-75/27.01.2021.

1 Introduction

Introduced for the first time by Schmid [1] in the fluid mechanics community, *dynamic mode decomposition* (DMD) has emerged as a leading technique to identify spatiotemporal coherent structures from high-dimensional data. Shortly after its introduction, it was shown by Rowley et al. in [2] close relation between the DMD and spectral analysis of the Koopman operator is shown, see also [3]. DMD analysis can be considered to be a numerical approximation to Koopman spectral analysis, and in this sense it is applicable to nonlinear dynamical systems.

Over the past decade, the popularity of DMD method has grown and it has been applied for a variety of dynamical systems in many different fields such as video processing [12], epidemiology [13], neuroscience [15], financial trading [16, 17, 18], robotics [14], cavity flows [4, 6] and various jets [2, 5].

Theoretical work on connections of DMD method with other methods, such as POD [4], Fourier analysis [10] and Koopman spectral analysis [2, 7, 11]. Theorems regarding the existence and uniqueness of DMD modes and eigenvalues can be found in [10]. For a review of the DMD literature, we refer the reader to [8, 9, 19].

The remainder of this work is organized as follows: in the rest of Section 1 we describe the DMD algorithm, in Section 2, we propose and discuss a new approach for DMD computation and in Section 3 we present examples demonstrating the new algorithm. The conclusion is in Section 4.

1.1 The Dynamic Mode Decomposition Algorithm

In this paragraph the DMD algorithm is briefly reviewed.

Standard definition

The standard definition of DMD consider a sequential set of data $Z = \{z_0, \ldots, z_m\}$, where each $z_k \in R^n$. The data could be from measurements, experiments or simulations collected at time t_i from a given nonlinear system, assume that the data are equispaced in time, with a time step $\triangle t$ and the collection time starts from t_0 to t_m. The main assumption of the method is that there exists a linear (unknown) matrix A relating z_k to the subsequent z_{k+1}:

$$z_{k+1} = Az_k. \tag{1}$$

The DMD modes and eigenvalues are intended to approximate the eigenvectors and eigenvalues of A. The method uses arrangement of the data set

into two large data matrices:

$$X = [z_0, \ldots, z_{m-1}] \quad \text{and} \quad Y = [z_1, \ldots, z_m]. \tag{2}$$

Then the algorithm proceeds as follows:

Algorithm 1: Standard DMD

Input: Data matrices X and Y, and rank r.
Output: DMD eigenvalues Λ and modes Φ
1: **Procedure** DMD(X,Y,r).
2: $[U, \Sigma, V] = SVD(X, r)$ *(Truncated r-rank SVD of X)*
3: $\tilde{A} = U^* Y V \Sigma^{-1}$ *(Low rank approximation of A)*
4: $[W, \Lambda] = EIG(\tilde{A})$ *(Eigen-decomposition of $\tilde{A}$)*
5: $\Phi = UW$ *(DMD modes of A)*
6: **End Procedure**

Exact DMD algorithm

A more general definition of DMD method is presented by Tu et al. in [8], where the data is collected as a set of n-dimensional vectors (x_k, y_k) (for $k = 1, \ldots, m$), in contrast to the sequential time series. Then the corresponding to (2) two sets of data are:

$$X = [x_1, \ldots, z_m] \quad \text{and} \quad Y = [y_1, \ldots, y_m]. \tag{3}$$

The algorithm introduced in [8] is nearly identical to Algorithm 1. The only difference is that the DMD modes (at step 5) are computed by the formula

$$\Phi = YV\Sigma^{-1}W. \tag{4}$$

The modes in (4) are often called *exact DMD modes*, because Tu et al. in [8] prove that these are exact eigenvectors of the matrix A. The modes in $\Phi = UW$ used in Algorithm 1 are referred to as *projected DMD modes* [4].

As a result of the presented algorithms, we can reconstruct the approximate dynamics of data set Z. For convenience the DMD eigenvalues λ_j can be converted to Fourier modes as $\omega_j = \ln(\lambda_j)/\triangle t$. Therefore the approximate solution at all times is given by

$$z_{DMD}(t) = \Phi \exp(\Omega t) b, \tag{5}$$

where the columns of Φ are the DMD modes, and $\Omega = diag\{\omega_j\}_{j=1}^r$ is a diagonal matrix with entries the corresponding eigenvalues ω_j. The vector

b determines the weighting of each of the r modes, so that $z_0 = \Phi b$. Then the vector $z_{DMD}(t)$ defines the state of the system at time t.

In the case of uniformly sampled $z(t)$, the presentation (5) at the sampling instants $t_k = k\triangle t$ is

$$z_{DMD}(k) = \Phi \Lambda^k b, \tag{6}$$

where $\Lambda = diag\{\lambda_j\}_{j=1}^{r}$, $b = \Phi^+ z_0$, and Φ^+ is the pseudo-inverse of Φ.

2 A new approach

Originally the DMD algorithm [1, 2] was formulated in terms of a companion matrix , which highlights its connections to the Arnoldi algorithm and to Koopman operator theory. Recall, that the main idea of DMD method is to assume the existence of a linear operator A with the properties described in (1). From (1) and (2) it follows

$$Y = AX. \tag{7}$$

If we assume that the data sequence $\{z_0, \ldots, z_m\}$ is sufficiently long, i.e. m is sufficiently large, then the vector z_m can be expressed as a linear combination of the independent sequence $\{z_i\}_{i=0}^{m-1}$. Then Y is related with X by

$$Y = XF + R, \tag{8}$$

where F is the Frobenius companion matrix and R is the residual matrix. It is then known that the eigenvalues of F, also referred to as the Ritz values, approximate some of the eigenvalues of the matrix A when $\|R\|_2 \to 0$. The objective is to minimize the residual:

$$F = argmin_F \|Y - XF\|.$$

To achieve this, we identify the singular value decomposition of matrix X

$$X = U\Sigma V^*, \tag{9}$$

where the unitary matrix U contains the proper orthogonal modes of X, the unitary matrix V is the right singular matrix of X, and the diagonal matrix Σ contains the singular values of X (where $(.)^*$ denotes the conjugate transpose). Then F is calculated by multiplying Y by the X pseudoinserve

$$F = X^+ Y = V\Sigma^{-1} U^* Y. \tag{10}$$

Relations (7)-(10) and $\|R\|_2 \to 0$ yield

$$A = XFX^+. \tag{11}$$

Then for the right hand side of (11), we obtain

$$XFX^+ = U\Sigma V^* FV\Sigma^{-1}U^* = U\Sigma\tilde{F}\Sigma^{-1}U^*, \tag{12}$$

where

$$\tilde{F} = V^* FV. \tag{13}$$

Let

$$\tilde{F} = W\Lambda W^{-1} \tag{14}$$

be the eigendecomposition of $\tilde{F}$. Then from (11), (12) and (14) we get the decomposition of the form

$$A = U\Sigma W\Lambda W^{-1}\Sigma^{-1}U^*,$$

or the equivalently

$$AU\Sigma W = U\Sigma W\Lambda\,.$$

Thus we showed that

$$\Phi = U\Sigma W$$

is the eigenvector matrix of A.

On the other hand, from (10) and (13) we get the following expression of $\tilde{F}$

$$\tilde{F} = \Sigma^{-1}U^* YV. \tag{15}$$

Now, we are ready to introduce the alternative algorithm for computing the DMD modes and eigenvalues.

Algorithm 2: Alternative DMD

Input: Data matrices X and Y, and rank r.
Output: DMD eigenvalues Λ and modes Φ
1: **Procedure** DMD(X,Y,r).
2: $[U, \Sigma, V] = SVD(X, r)$ *(Truncated r-rank SVD of X)*
3: $\tilde{F} = \Sigma^{-1}U^*YV$ *(Low rank approximation of F)*
4: $[W, \Lambda] = EIG(\tilde{F})$ *(Eigen-decomposition of $\tilde{F}$)*
5: $\Phi = U\Sigma W$ *(DMD modes of A)*
6: **End Procedure**

From (14) and (15) we get the projection of Y onto a basis formed by the eigenmodes $U\Sigma W$

$$Y = (U\Sigma W)\Lambda(W^{-1}V^*), \tag{16}$$

which is equivalent to

$$Y = (XVW)\Lambda(W^{-1}V^*).$$

From expression (16), one obtains the contribution of each dynamic mode to Y:

- its amplitude is given by the norm of corresponding column vector of $U\Sigma W$;
- its frequency and damping are provided by the eigenvalues in Λ.

Theorem 1. *Let (λ, w), with $\lambda = 0$, be an eigenpair of $\tilde{F}$ defined by (13) and let assume that the relation $A = XFX^+$ defined by (11) is fulfilled, then the corresponding eigenpair of A is (λ, φ), where*

$$\varphi = YVw.$$

Proof. By using the SVD decomposition (9) and the pseudoinverse of X

$$X^+ = V\Sigma^{-1}U^*$$

we get the expression

$$A = YX^+ = YV\Sigma^{-1}U^*.$$

Let now express $A\varphi$

$$A\varphi = YV\Sigma^{-1}U^*YVw$$

which implies, by using (15)

$$A\varphi = YV\tilde{F}w = YVw\lambda = \lambda\varphi.$$

In addition, $\varphi \neq 0$, since if $YVw = 0$, then $\Sigma^{-1}U^*YVw = \tilde{F}w = 0$, which implies $\lambda = 0$. Hence, φ is an eigenvector of A with eigenvalue λ. The proof is completed.

Now, we can formulate an alternative version of Algorithm 2:

Algorithm 3 is almost identical to Algorithm 2. In fact, the two algorithms differs only in computation of the DMD modes.

Algorithm 3: Alternative DMD-2

Input: Data matrices X and Y, and rank r.
Output: DMD eigenvalues Λ and modes Φ
1: **Procedure** DMD(X,Y,r).
2: $[U, \Sigma, V] = SVD(X, r)$ *(Truncated r-rank SVD of X)*
3: $\tilde{F} = \Sigma^{-1} U^* Y V$ *(Low rank approximation of F)*
4: $[W, \Lambda] = EIG(\tilde{F})$ *(Eigen-decomposition of $\tilde{F}$)*
5: $\Phi = YVW$ *(DMD modes of A)*
6: **End Procedure**

3 Numerical examples

To illustrate the algorithms introduced in Section 2, we consider two simple examples with mixed spatiotemporal signals. Also, our objective is to compare the results with the results of standard DMD algorithms (presented in [1, 8]).

Example 1

Let us have two signals of interest

$$f_1(x,t) = \text{sech}(x+3)\exp(i2.3t)$$

and

$$f_2(x,t) = 2\text{sech}(x)\tanh(x)\exp(i2.8t),$$

and the mixed signal is

$$f(x,t) = \text{sech}(x+3)\exp(i2.3t) + 2\text{sech}(x)\tanh(x)\exp(i2.8t). \tag{17}$$

This example is demonstrated in [9] with the original DMD algorithm.

The individual spatiotemporal signals $f_1(x,t)$ and $f_2(x,t)$ are illustrated in Figure 1 (i)-(ii). The two frequencies present are $\omega_1 = 2.3$ and $\omega_2 = 2.8$, which have distinct spatial structures. The mixed signal $x(t) = f_1(x,t) + f_2(x,t)$ is illustrated in Figure 1 (iii). We perform a rank-2 decomposition (5) by using the three mentioned algorithms: *Algorithm 1*, *Algorithm 2* and *Algorithm 3*. The corresponding three approximate reconstructions of $x(t)$ are shown in Figure 1 (iv)-(vi), respectively. The reconstruction is almost perfect, with the DMD modes and spectra closely matching those of the underlying signals $f1(x,t)$ and $f2(x,t)$. We can say that the alternative algorithms (*Algorithm 2* and *Algorithm 3*) produce the same result as the exact DMD procedure (*Algorithm 1*).

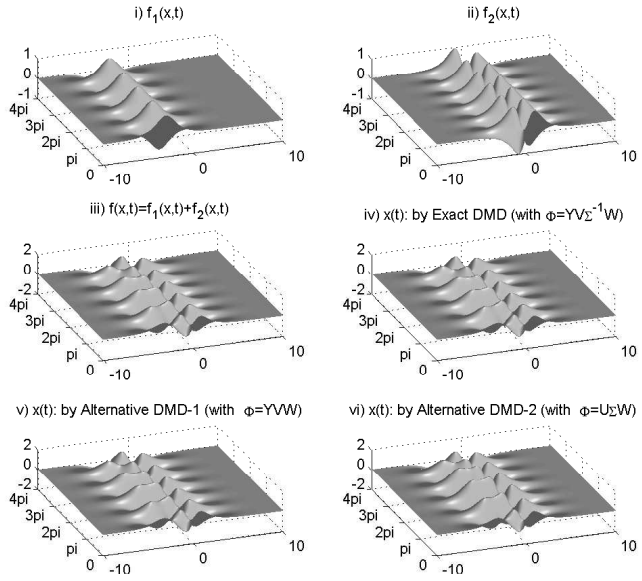

Figure 1: Spatiotemporal dynamics of two signals (i) $f_1 = (x,t)$ and (ii) $f_2 = (x,t)$ of Example 1 that are mixed in (iii) $x(t) = f(x,t) = f_1(x,t) + f_2(x,t)$. The *exact* $x_{DMD}(t)$ is shown in panel (iv), *alternative-1* $x_{DMD}(t)$ is shown in (v) and *alternative-2* $x_{DMD}(t)$ is shown in (vi).

Example 2: Translational and rotational invariances

The DMD method, is based on an underlying SVD that extracts correlated patterns in the data. It is well known that the main weakness of such SVD-based approaches is the inability to efficiently handle invariances in the data. Specifically, translational and/or rotational invariances of low-rank objects embedded in the data are not well captured. To demonstrate the impact of the translation, we consider again Example 1, where the one of the signals is translating at a constant velocity across the spatial domain. The two signals of interest are

$$f_1(x,t) = \mathrm{sech}(x+6-t)\exp(i2.3t)$$

and

$$f_2(x,t) = 2\mathrm{sech}(x)\tanh(x)\exp(i2.8t),$$

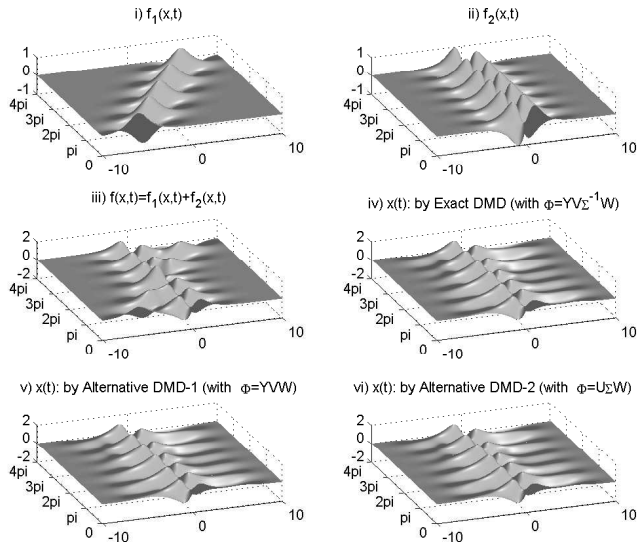

Figure 2: Spatiotemporal dynamics with translation Example 2. The two signals (i) $f_1 = (x,t)$, (ii) $f_2 = (x,t)$ and the mixed $x(t) = f(x,t) = f_1(x,t)+f_2(x,t)$ (iii). The *exact* $x_{DMD}(t)$ is shown in panel (iv), *alternative-1* $x_{DMD}(t)$ is shown in (v) and *alternative-2* $x_{DMD}(t)$ is shown in (vi).

and the mixed signal is

$$f(x,t) = \text{sech}(x+6-t)\exp(i2.3t) + 2\text{sech}(x)\tanh(x)\exp(i2.8t).$$

As before, the two frequencies present are $\omega_1 = 2.3$ and $\omega_2 = 2.8$, with given corresponding spatial structures. The individual spatiotemporal signals $f_1(x,t)$ and $f_2(x,t)$, along with the mixed solution $x(t) = f(x,t) = f_1(x,t) + f_2(x,t)$, are illustrated in Figure 1 (i)-(iii), respectively.

We perform again decomposition (5) by using the three mentioned algorithms: *Algorithm 1*, *Algorithm 2* and *Algorithm 3*. The corresponding three approximate reconstructions of $x(t)$ are shown in Figure 2 (iv)-(vi), respectively.

In this case, we use rank-2, rank-5, and rank-10 reconstructions. The rank-2 and rank-5 reconstruction are no able to characterize the dynamics due to the translation. Although the dynamics are constructed from a two-mode interaction, the reconstruction now requires approximately 10 modes to get the right dynamics. This artificial inflation of the dimension is a result of the inability of SVD to capture translational invariances and correlate across snapshots of time. Once again the results in last three panels Figure 2 (iv)-(vi) are identical.

4 Conclusion

The purpose of this study was to present a new approach for computing approximate DMD modes and eigenvalues. As a result, we have introduced two algorithms, alternative procedures for executing the DMD decomposition. We demonstrate the performance of the presented algorithms with numerical examples. From the obtained results we can conclude that the introduced approach gives identical results with those of the *exact DMD method* [8].

References

[1] P. J. Schmid and J. Sesterhenn. Dynamic mode decomposition of numerical and experimental data. In 61st Annual Meeting of the APS Division of Fluid Dynamics. American Physical Society, November 2008.

[2] C. W. Rowley, I. Mezić, S. Bagheri, P. Schlatter, and D. S. Henningson. Spectral analysis of nonlinear flows. J. Fluid Mech., 641:115-127, December 2009.

[3] I. Mezić. Spectral properties of dynamical systems, model reduction and decompositions. Nonlin. Dynam., 41(1-3):309-325, August 2005.

[4] P. J. Schmid. Dynamic mode decomposition of numerical and experimental data. J. Fluid Mech., 656:5-28, August 2010.

[5] P. J. Schmid. Application of the dynamic mode decomposition to experimental data. Exp. Fluids, 50(4):1123-1130, April 2011.

[6] A. Seena and H. J. Sung. Dynamic mode decomposition of turbulent cavity ows for selfsustained oscillations. Int. J. Heat Fluid Fl., 32(6):1098-1110, December 2011.

[7] I. Mezić. Analysis of fluid flows via spectral properties of the Koopman operator. Annu. Rev. Fluid Mech., 45:357-378, 2013.

[8] Jonathan H. Tu, Clarence W. Rowley, Dirk M. Luchtenburg, Steven L. Brunton, J. Nathan Kutz. On dynamic mode decomposition: Theory and applications. Journal of Computational Dynamics, 2014, 1 (2) : 391-421. doi: 10.3934/jcd.2014.1.391

[9] J. Nathan Kutz, Steven L. Brunton, Bingni W. Brunton, and Joshua Proctor (2016). Dynamic Mode Decomposition: Data-Driven Modeling of Complex Systems, SIAM 2016, ISBN 978-1-611-97449-2, pp. 1-234.

[10] K. K. Chen, J. H. Tu, and C. W. Rowley. Variants of dynamic mode decomposition: Boundary condition, Koopman, and Fourier analyses. J. Nonlinear Sci., 22:887-915, 2012.

[11] S. Bagheri, Koopman-mode decomposition of the cylinder wake, J. Fluid Mech., vol. 726, pp. 596-623, 2013.

[12] J. Grosek, J. Nathan Kutz, Dynamic Mode Decomposition for Real-Time Background/Foreground Separation in Video, arXiv: 1404.7592.

[13] J. L. Proctor and P. A. Eckhoff, Discovering dynamic patterns from infectious disease data using dynamic mode decomposition, International health, 7 (2015), pp. 139-145.

[14] E. Berger, M. Sastuba, D. Vogt, B. Jung, and H. B. Amor, Estimation of perturbations in robotic behavior using dynamic mode decomposition, Journal of Advanced Robotics, 29 (2015), pp. 331-343.

[15] B. W. Brunton, L. A. Johnson, J. G. Ojemann, AND J. N. Kutz, Extracting spatialtemporal coherent patterns in large-scale neural recordings using dynamic mode decomposition, Journal of Neuroscience Methods, 258 (2016), pp. 1-15.

[16] J. Mann and J. N. Kutz, Dynamic mode decomposition for financial trading strategies, Quantitative Finance, (2016), pp. 1-13.

[17] Ling-xiao Cui, Wen Long, 2016. "Trading strategy based on dynamic mode decomposition: Tested in Chinese stock market," Physica A: Statistical Mechanics and its Applications, Elsevier, vol. 461(C), pages 498-508.

[18] D. P. Kuttichira, E. A. Gopalakrishnan, V. K. Menon and K. P. Soman, "Stock price prediction using dynamic mode decomposition," 2017 International Conference on Advances in Computing, Communications and Informatics (ICACCI), Udupi, India, 2017, pp. 55-60, doi: 10.1109/ICACCI.2017.8125816.

[19] Zhe Bai, Eurika Kaiser, Joshua L. Proctor, J. Nathan Kutz, Steven L. Brunton, Dynamic Mode Decomposition for CompressiveSystem Identification, AIAA Journal, Vol. 58, No. 2, February 2020, pp. 561-574.